Artificial Potential Field and Sliding Mode Strategies for Proximity Operations with Obstacle Avoidance

2018 15th International Workshop on Variable Structure Systems (VSS)
Graz University of Technology, Graz, Austria, July 9-11, 2018

Artificial Potential Field and Sliding Mode Strategies for Proximity Operations with Obstacle Avoidance

N. Bloise[1], E. Capello[2], H. Park [3], E. Punta[4] and M. Romano[5]

Abstract— **This paper presents a combination of guidance and control algorithms, for spacecraft proximity operations in presence of multiple obstacles. The guidance algorithm is based on the theory of artificial potential field (APF) and the control algorithm is based on the theory of sliding mode control (SMC). The effects of both uncertainties and external disturbances are considered in this research. The proposed strategy is validated both by simulations and by experiments on a real testbed. The proposed algorithm appears to be suitable for autonomous, real-time control of complex maneuvers with a minimum on-board computational effort. It is also able to avoid obstacles while avoiding the local minimum issues in APF algorithms.**

I. Introduction

Autonomous rendezvous and proximity operations are essential for automated missions to assembly and repair a satellite, to bring supplies to the International Space Station (ISS), involving different type of spacecraft. In the last five years, recent studies on proximity operations and close-range maneuvers have been deeply studied, and this automated mission has to be successfully completed by relying on a robust flight software. The research proposed in this paper is based on the design and validation of the on-board software, able to generate an optimized path and to detect the presence of unexpected events/objects along the trajectory and ensure its avoidance.

The focus of the recent space missions is on the study of obstacle avoidance algorithms, many scenarios involve operations to be performed either near to large space structures or, due to the increase of space debris, in proximity of obstacles [1]. For this reason, the objective of the present work is the design and implementation of guidance and control algorithms, able to avoid obstacles and able to be implemented in real-time. The approach proposed for the guidance algorithm is based on the theory of artificial potential fields with paraboloid-based and hyperbolic-based shapes. For the control algorithms, a first-order sliding mode controller (SMC) is proposed, motivated by the intrinsic nature of the thrusters, which cannot provide continuously modulated thrusts and can only be switched on and off.

In variable structure control (VSC) systems [2], [3], the control law is a function of the system state and changes among the possible structures according to some suitably defined rules. In particular, in SMC systems a switching function is designed, which implicitly defines a sliding surface corresponding to the points in the state space in which the switching function is zero. At any time, the structure applied by the control law depends on the position of the state with respect to the sliding surface. When a sliding motion is established, the closed-loop system is in sliding mode and its trajectories are constrained on the sliding surface. In sliding mode, the switching function defines the structure of the control law at any time, depending on the position of the state. SMC is a general method for designing controllers for uncertain systems and provides invariance to matched uncertainties, that is, uncertainties that affect the dynamics of the system acting in the input channels and insensitivity to parameters variations.

The main features of SMC are the robustness properties against matched and bounded external disturbances and parameter variations, as well as the simplicity in design. Commonly, the use of discontinuous control laws, which commute among the allowed control structures, and the related chattering phenomenon are considered as the main drawbacks for the practical implementation in real systems of SMC.

In this paper a first-order SMC is proposed for the control of the spacecraft maneuver. Usually, this kind of controller is not implemented in mechanical systems, since the designed control inputs, which are forces, thrusts, and torques, are required to be discontinuous. In the considered case the spacecraft is actuated by discontinuous mono-directional thrusters, therefore the first-order SMC results to be the most suitable to be implemented due to the intrinsic technical characteristics of the used actuators, which cannot provide continuously modulated thrusts and can only be switched on and off.

As introduced before, the SMC control algorithm is combined with a suitable designed guidance algorithm, focusing on proximity operations. Even if in the last years, more attention is dedicated to proximity maneuvers as in [4], nevertheless, usually, no disturbances or model uncertainties are included. Instead in [5] the proximity maneuver is clearly described, in which the Chaser is driven to a certain fixed position along the docking port and the relative attitude is

[1]N. Bloise is with the Department of Mechanical and Aerospace Engineering, Politecnico di Torino, Corso Duca degli Abruzzi 24, 10129 Torino, Italy, (nicoletta.bloise@polito.it).

[2] E. Capello is with the Department of Mechanical and Aerospace Engineering and with the CNR–IEIIT, Politecnico di Torino, Corso Duca degli Abruzzi 24, 10129 Torino, Italy, (elisa.capello@polito.it).

[3]H. Park is with the Department of Mechanical and Aerospace Engineering, New Mexico State University, Las Cruces, NM, USA, (hjpark@nmsu.edu).

[4] E. Punta is with the Institute of Electronics, Computer and Telecommunication Engineering, National Research Council of Italy (CNR-IEIIT), Torino, Italy, (elisabetta.punta@ieiit.cnr.it), and with the International Telematic University UniNettuno, Rome, Italy.

[5] M. Romano is with the Department of Mechanical and Aerospace Engineering, Naval Postgraduate School, Monterey, CA, USA, (mromano@nps.edu).

synchronized for subsequent docking operations. In [6] the Artificial Potential Function method (APF)-based repulsive functions provide collision avoidance for both fixed and moving obstacles, but it is used as control algorithm for the repulsive force. Instead, in our paper the APF-based guidance algorithm is designed for the definition of the desired speed and a SMC two-channel controller is implemented as control algorithm.

A similar research based on the real-time on-board execution of APF as a guidance scheme is analyzed in [7]. More recently, interesting applications of APF as guidance algorithms are proposed in [8]. In [8] an adaptive artificial field for proximity operations is considered and the computational efficiency is proven in an experimental testbed. In this case, the APF algorithm is used as guidance and control (GC) system and an "ad hoc" field is generated. In our work, feedback control based on SMC theory is designed for tracking the gradient, generated by the APF algorithm. Our idea is to propose a method able to guarantee real-time implementations on a testbed, including hardware limitations on the control design.

In our case, both position and attitude dynamics are controlled by a conventional first-order SMC, that is, the most suitable, due to the thrusters, for which the designed control signals are discontinuous. The advantage of this combination of GC autonomous system is twofold: (i) an autonomous way for the desired path is designed with a low computational effort, and (ii) an on-line update and control of the path is guaranteed, in particular in presence of obstacles. As in [9], a simple shape APF algorithm is proposed to have a reliable method (the same field for all the maneuver) and to avoid obstacles, even for the experimental testbed with multiple obstacle scenario. Moreover, external disturbances are also considered, to demonstrate the robustness of the proposed controller. A similar problem was already considered in [9]. Nevertheless, here important original contributions with respect to the previous paper are proposed: (i) a dynamic variation of the safety radius of the obstacle, and (ii) a different sliding surface is designed for the position and attitude dynamics. Moreover, the proximity operations maneuver is performed and validated both in simulations and on an experimental testbed.

The paper is organized as follows. In Section II the considered maneuver is described and analyzed, focusing on the spacecraft dynamics. The description of the artificial potential field as guidance is provided in Section III, while the control strategies are presented in Section IV. A baseline scenario is described in Section V, including experimental tests. A multiple obstacle scenario is presented in Section VI. Finally, some concluding remarks are proposed in Section VII.

II. Problem Setup

The developed algorithms are experimentally tested and evaluated on the NPS-POSEIDYN[1] test bed [10] at the Spacecraft Robotics Laboratory. The experimental setup includes floating spacecraft simulators (FSS), a polished granite table, a ground station computer, and a Vicon motion capture system, as shown in Figure 1.

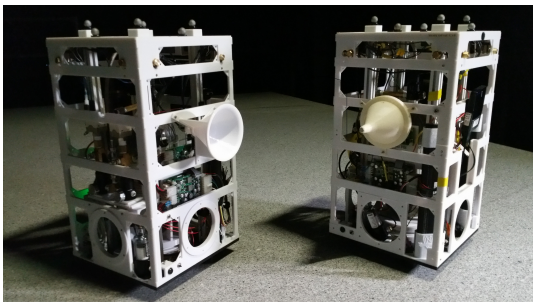

Fig. 1. The Target (left) and Chaser (right) FSS, [8].

The floating surface is a 4-by-4 meter and 15 ton granite monolith. The FSS simulators, approximately 10 kg vehicles, float over the granite monolith surface via three air bearings. The relative navigation problem is solved by using the Vicon motion capture system provides the relative navigation information such as accurate position and orientation data using ten overhead cameras that track reflectors mounted on the FSS. This data is processed on an external computer and streamed to the FSS using a Wi-Fi connection to provide a full state estimate.

The developed controller is included in the guidance, navigation, and control (GNC) algorithms based on a MATLAB/Simulink environment including the sensor and actuator blocks. The MATLAB/Simulink model is then cross-compiled and transferred to the FSS simulator.

The FSS dynamic model consists of three double integrators, two translational and one rotational degree-of-freedom (DoF). The dynamics is described in a state-space formulation as

$$\dot{\zeta} = A\zeta + B\mathrm{u}, \tag{1}$$

with the state and control matrices

$$A = \begin{bmatrix} 0_{3\times3} & \mathbb{I}_3 \\ 0_{3\times3} & 0_{3\times3} \end{bmatrix}, \quad B = \begin{bmatrix} & 0_{3\times3} & \\ \frac{1}{m} & 0 & 0 \\ 0 & \frac{1}{m} & 0 \\ 0 & 0 & \frac{1}{I_z} \end{bmatrix}, \tag{2}$$

where m and I_z are the mass and moment of inertia about the vertical axis of the FSS, respectively and the state vector is $\zeta = [x, y, \theta]^T \in R^3$. The control vector $\mathrm{u} = [u_x, u_y, u_\theta]^T \in R^3$ is exploited by thrusters.

The actuation system exploits thrusters and can exert mono-directional actions, that is they can apply to the Chaser thrusts of given magnitude and along fixed directions, which depend on how and where the thrusters have been assembled in the system (their orientations and application points).

III. Artificial Potential Field as Guidance Algorithms

An analytical method and a computational-efficient algorithm is proposed to reach the Target in a safe way and to

[1]POSEIDYN stands for Proximity Operation of Spacecraft: Experimental hardware-In-the-loop DYNamic simulator

"fast" adjust the trajectory when the Chaser is close to the obstacle. When a spacecraft is moving in an environment with obstacles, sensors and on-board GC algorithms have to manage the rendezvous procedure in an autonomous way as quickly as possible. Moreover, the GC algorithm sends inputs to the spacecraft to perform almost impulsive maneuvers, including external disturbances and uncertainties. The APF strategy, even in presence of obstacles, allows the reduction of the fuel consumption and of the computational effort, guaranteeing a simple on-line implementation. This method constructs step by step the artificial potential field and, in the meantime, the desired speed field to drive the spacecraft to the goal of each phases.

A. Definition of the APF

An attractive paraboloid APF and a repulsive hyperbolic APF are considered. The guidance algorithm gains and the APF algorithms are defined to obtain a decreasing of the Chaser speed, as it approaches the goal (Target spacecraft).

As in [9], the attractive potential field is evaluated as

$$U_a(\mathrm{x}) = \tfrac{1}{2} k_a ||e(\mathrm{x})||^2, \tag{3}$$

where k_a is the proportional positive gain of the attractive gradient, $e(\mathrm{x})$ is the error in position, $\mathrm{x} = [x, y]^T \in R^2$ are the positions in LVLH frame. The connected attractive force $f_a(\mathrm{x})$ is obtained by the negative gradient of this attractive

$$f_a(\mathrm{x}) = - \bigtriangledown U_a(\mathrm{x}). \tag{4}$$

To avoid the obstacles, a repulsive potential field is defined, one for each obstacle ($i = 1, \dots N_{obs}$ with N_{obs} number of obstacles)

$$U_{r,i}(\mathrm{x}) = \begin{cases} \frac{k_{r,i}}{\gamma} (\frac{1}{\eta_i(\mathrm{x})} - \frac{1}{\eta_{0,i}(\mathrm{x})})^\gamma & \text{if } \eta_i(\mathrm{x}) \leq \eta_{0,\mathrm{i}}(\mathrm{x}) \\ 0 & \text{if } \eta_i(\mathrm{x}) > \eta_{0,\mathrm{i}}(\mathrm{x}) \end{cases}, \tag{5}$$

where $k_{r,i}$ is the proportional positive gain of the repulsive field, $\gamma = 2$ is defined for the hyperbolic field, $\eta_i(\mathrm{x}) = \min_{\mathrm{x_{obs}} \in \mathrm{CO^i}} ||\mathrm{x} - \mathrm{x_{obs}}||$, $\mathrm{x_{obs}} \in \mathrm{R}^2$ is the obstacle position, and $\eta_{0,i}(\mathrm{x})$ is the safety radius, that is the distance of influence of obstacles. CO^i is the convex set of obstacles. A repulsive field is defined for each obstacle and assumed convex.

As before, the repulsive force is

$$f_{r,i}(\mathrm{x}) = \begin{cases} \frac{k_{r,i}}{\eta_i^2(\mathrm{x})} \left(\frac{1}{\eta_i(\mathrm{x})} - \frac{1}{\eta_{0,i}(\mathrm{x})} \right)^{\gamma - 1} \bigtriangledown \eta_i(\mathrm{x}) & \text{if } \eta_i(\mathrm{x}) \leq \eta_{0,\mathrm{i}}(\mathrm{x}) \\ 0 & \text{if } \eta_i(\mathrm{x}) > \eta_{0,\mathrm{i}}(\mathrm{x}) \end{cases}. \tag{6}$$

As previously stated, the radius $\eta_{0,i}$ for $i = 1, \dots, N_{obs}$ is the safety radius. This means that the Chaser starts to sense the obstacle when they are $\eta_{0,i}$ m far from each other.

In our case, a dynamic variation of this radius is considered, to obtain a smooth trajectory and avoiding singular lines. An heuristic measure is proposed for the evaluation of the dynamic radius. As in [11],

$$R_{dyn} = \max \left(R - \frac{\dot{x}_r |\dot{x}_r|}{2 \epsilon_s a_{max}}, 0 \right), \tag{7}$$

$R = \eta_{0,i}$ is the nominal safety radius, $\dot{x}_r$ radial velocity component directed toward the security circle center (considered negative when approaching the obstacle), and $\epsilon_s \in (0, 1]$ is a safety factor. The acceleration command is $a_{max} = \frac{T_{max} - \bar{f}}{\sqrt{2} m_c}$, in which T_{max} is the maximum thrust provided by thrusters, $\bar{f} = 10^{-3}$ N is related to the actuation system uncertainties, and m_c is the Chaser mass. The uncertainty $\bar{f}$ is a random variable with known distribution, confined in a set related to the experimental setup thrusters.

The applied artificial potential field is the sum of the attractive and repulsive part

$$U_t(\mathrm{x}) = U_a(\mathrm{x}) + \sum_{i=1}^{N_{obs}} U_{r,i}.$$

A unit vector of the potential field is evaluated to assign the direction of the desired speed

$$E_U = \frac{f_a(\mathrm{x}) + f_{r,i}(\mathrm{x})}{|| \bigtriangledown U_t(\mathrm{x})||},$$

thus the desired speed $\dot{\mathrm{x}}_d = [\dot{x}_d, \dot{y}_d]^T \in R^2$ is

$$\dot{\mathrm{x}}_d = \dot{x}_{d,max} E_U, \tag{8}$$

where $\dot{x}_{d,max}$ is the maximum speed to perform the maneuver, that is scalar and equal along the two axes.

B. Local minimum evaluation

Even if a dynamic radius is considered and a smooth path is obtained, the problem of local minimum, that usually affects APF algorithms [12], can be observed. Moreover, since the attractive and repulsive gains are fixed, local minimum and oscillation problems can arise.

If $|f_a(\mathrm{x}) + f_r(\mathrm{x}, i)| \geq \epsilon$, with $i = 1, \dots, N_{obs}$ for any small $\epsilon \in [0, 1] \geq 0$, the robot is in a local minimum and the attractive and repulsive forces are (almost) equal and opposite. To avoid this condition, a rotation of the attractive force is proposed, including the constraints related to nominal security radius and to obtain a smooth path. Thus, the angle of rotation is evaluated as

$$\beta = \arctan \left(\frac{1}{||\mathrm{x} - \mathrm{x_{obs}}|| - R} \right). \tag{9}$$

According to Eqs. (4) and (9), the new attractive force is

$$f_{a,new} = \begin{bmatrix} \cos\beta & -\sin\beta \\ \sin\beta & \cos\beta \end{bmatrix} f_a,$$

which means a deviation of the attractive force evaluated in Eq. (4) of the β angle.

IV. Gradient Tracking via Sliding Mode Control

As deeply discussed in [13] and described for spacecraft maneuvers in [14], internal and external disturbances affect the system due to the real implementation of the control laws, as well as due to the external environment; all these uncertain and perturbing terms must be taken into account. Sliding mode methods can counteract uncertainties and disturbances, if the perturbations affecting the system are matched and bounded (first-order SMC) or smooth matched disturbances with bounded gradient (second-order SMC), [15], [16].

The proposed control strategy consists of two SMC suitably designed for the spacecraft. A first-order sliding mode is designed, motivated by the intrinsic nature of the thrusters, which cannot provide continuously modulated thrusts and can only be switched on and off.

The technical characteristics of the actuators, together with the fact that at any time the APF algorithms identify the desired speed vector for the spacecraft, make the use of a first-order SMC particularly suitable to design the controller. In fact, first-order SMC is able to guarantee the finite time tracking of the desired speed and of the corresponding position despite the uncertainties and the disturbances affecting the system.

The input vector $u_{\mathrm{x}} = [u_x, u_y]^T \in R^2$ is designed according to the following first-order sliding mode control strategy

$$u_{\mathrm{x}} = -B_{\mathrm{x}}^{-1} K \mathrm{sgn}(\sigma_{\mathrm{x}}), \tag{10}$$

where $B_{\mathrm{x}}^{-1} = mI_2$, $K = nT_{max}$, and $n = 2$ reflects the fact that two thrusters are switched on simultaneously. σ_{x} represents the designed sliding output for the position tracking. In general, the control gain K in (10) must guarantee that the sliding motion on the desired sliding manifold is reached and maintained.

The sliding output $\sigma_{\mathrm{x}} = [\sigma_x, \sigma_y]^T \in R^2$, which is the switching function in the controller (10), is

$$\sigma_{\mathrm{x}} = \dot{\mathrm{x}} - \dot{\mathrm{x}}_d, \tag{11}$$

where $\dot{\mathrm{x}}_d = \dot{x}_{d,max} E_U \in R^2$ is the vector of the desired speed, evaluated with the APF algorithms (see Eq. 8). Therefore, this desired vector includes the evaluation of the unit vector affected by APF and can guarantee a slow motion in the area of high curvature, as discussed by [11]. The vector $\dot{\mathrm{x}} = [\dot{x}, \dot{y}]^T$ is the actual speed vector of the Chaser. The sliding controller for the attitude dynamics is a first-order one, because the actuation system is provided by thrusters (discontinuous input) and it is designed as

$$u_\theta = -I_z K \mathrm{sgn}(\sigma_\theta), \tag{12}$$

where $K = nT_{max}$, as in the previous case. The sliding output σ_θ, which is the switching function related to the attitude dynamics, is

$$\sigma_\theta = c_{\dot{\theta}}(\dot{\theta} - \dot{\theta}_d) + c_\theta(\theta - \theta_d), \tag{13}$$

where $c_{\dot{\theta}}$ and c_θ are scalar and constant values, $\dot{\theta}_d$ and θ_d are the angular velocity and the position of the Target.

V. Baseline Scenario

In this section experimental results with a single obstacle are presented. The FSS are custom-designed vehicles that emulate orbital spacecraft moving in close proximity of another vehicle or object (see Figure 1), as described in Section II. The air bearings use compressed air, delivered by an onboard tank, to lift the FSS approximately 5 μm, creating an air film between the vehicle and the granite surface that eliminates their direct contact. To propel the FSS, the vehicles are equipped with eight cold-gas thrusters, mounted in couple to each corner of the upper part of the vehicle, each one providing maximum thrust of 0.15 N.

A serial interface is used to communicate with an on-board Fiber-Optic Gyroscope which provides angular velocity measurements at a 100 Hz rate. Hence, the POSEIDYN setup is able to provide full-state estimate. Two 95 Wh lithium-ion batteries and a battery management module regulate the electrical power to the FSS. Whereas, a Wi-Fi module provides the FSS with wireless communication capabilities with other FSS and the ground station. Furthermore, once the location of the FSS is determined by the Vicon system, an external computer streams the telemetry data to the FSS using the Wi-Fi link. The main FSS physical properties are resumed in Table I, in terms of mass, geometry, and Moment Of Inertia (MOI). Additional details are provided in [10].

TABLE I
Summary of relevant FSS Physical Properties, [8].

Parameter	Value
Dry Mass [kg]	9.465 ± 0.001
Wet Mass [kg]	9.882 ± 0.001
Dimensions [m]	$0.27 \times 0.27 \times 0.52$
MOI [kg·m^2]	0.2527

To clearly understand the real-time feasibility of the proposed approach, the experimental tests performed for this first phase of the research are with a nominal radius and a single fixed obstacle, along the connection line between the Chaser and the Target. A sample time of 1 Hz is considered for the attitude dynamics, to avoid high fuel consumption, and of 50 Hz for the position dynamics. Strict conditions are required to perform the docking. The navigation filter is working at 50 Hz. The results of two experimental tests are included in this paper, with different initial conditions of the Chaser, as in Fig. 2. The variation of the thruster force is in Fig. 3. The solid line indicates the end of the experiments. Target position is evaluated by the system.

VI. Multi Obstacle Scenario

A detailed simulator of the NPS testbed described in Sections II and V is modeled, hardware constraints and limitations on the actuation system are included. In the section, the proximity operations maneuver with multiple obstacles and with different radius is analyzed. As described in Sections II and V, the Chaser has a mass of 10 kg and the initial conditions are ([3.5, 3.5] m) with a zero angle of

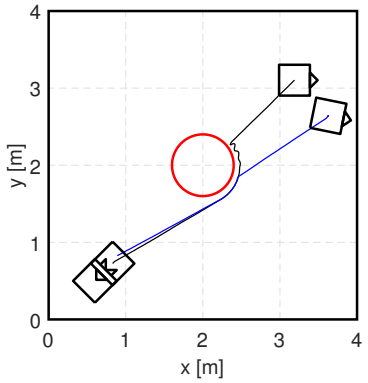

Fig. 2. Experimental tests with different initial conditions. Trajectory on x-y plane.

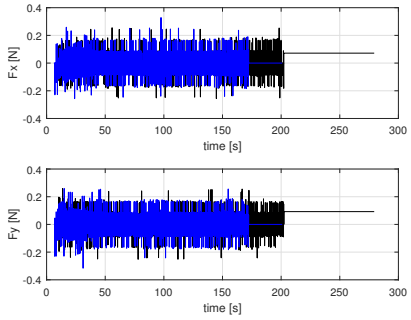

Fig. 3. Experimental tests with different initial conditions: force.

attitude. Instead the Target is considered in a fixed position, that is ([0.5, 0.5] m), with an attitude angle of $\frac{\pi}{4}$. The simulation tests are stopped when the final Target position is reached, since the docking is ensured by an attractive force generated by the magnets on the docking interface. The angular velocity of the Target is considered zero and the position of the Target is fixed. The same sample times defined in Section V are used for performing the simulations.

In detail, two case studies are analyzed.

– **Case 1:** The first case is $R_1 + R_2 > d$, R_1 is the radius of the first obstacle, R_2 is the radius of the second obstacle, and d is the distance between the two obstacle centers. The simulations are performed considering that the sum of the nominal safety radius of the two obstacles is greater than the distance between the two obstacle centers. In this case, to reduce the fuel consumption, the two obstacles are reduced to one obstacle with radius $(\frac{R_1+R_2}{2} + \frac{d}{2})$. A dynamic radius is considered: (i) to guarantee that the Chaser does not enter into the nominal security radius, and (ii) a smooth path is obtained. The trajectory is in Fig. 4. The Chaser is able to dock with the Target and to avoid the obstacle in a smoothing way. The sliding surfaces provided by the SMC, for both the position and attitude control, are visualized in Fig. 5 and in Fig. 6. The variation of the sliding surface is due to the presence of the obstacle. A null sliding output is guaranteeing at the end of the maneuver. As from Fig. 6, even if the attitude controller (1 Hz) is slower than the position one (50 Hz), the desired attitude is obtained after about 20 sec and is maintained for all the maneuver, until the docking.

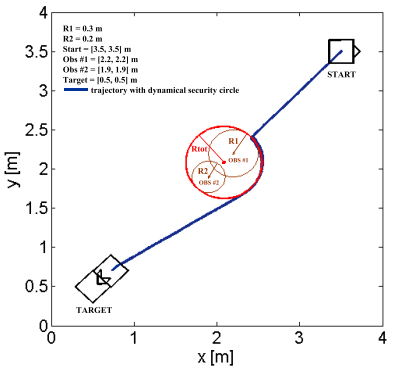

Fig. 4. Trajectory on x-y plane (case 1)

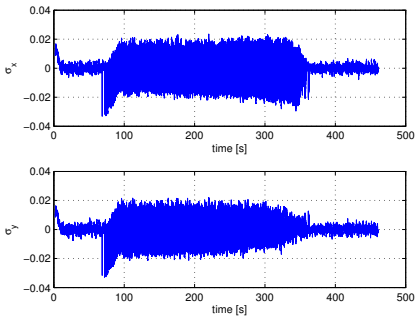

Fig. 5. Sliding surface for the position dynamics (case 1)

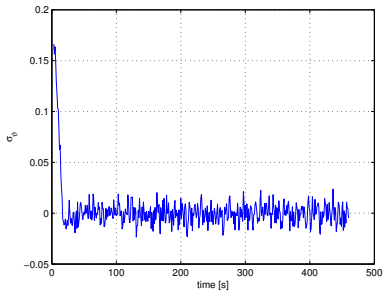

Fig. 6. Sliding surface for the attitude dynamics (case 1)

– **Case 2:** The second case is $R_1 + R_2 < d$. In this case, two obstacles are considered, with different radius, but without any intersection between the obstacles, this means that the closest obstacle is the one considered for the evaluation of the repulsive force. As in Fig. 7, the Chaser moves through the two obstacles and the trajectory obtained by the dynamic radius ensures the safety requirements. The sliding surfaces are in Fig. 8 and in Fig. 9. As for the previous case, the sliding output for the position dynamics is zero at the end of the

maneuver, but it is different from zero, if approaching the obstacles. For the attitude sliding surface (Fig. 6), even if the attitude controller (1 Hz) is slower than the position one (50 Hz), the desired attitude is obtained after about 20 sec and is maintained during the maneuver, until the docking.

Remark: *The applied control signals are designed by the (10) and (12) first-order SMC strategies. According to the exploited actuation system, based on discontinuous mono-directional thrusters, higher-order SMC techniques were not chosen to control the Chaser. Therefore, as expected, the chattering phenomenon arises in both experiments and simulation results, see Figs. 3, 5, 6, 8, 9. Moreover, in Fig. 5, it can be noted that chattering is more evident in the phase, particularly affected by disturbances, when the Chaser is avoiding an obstacle.*

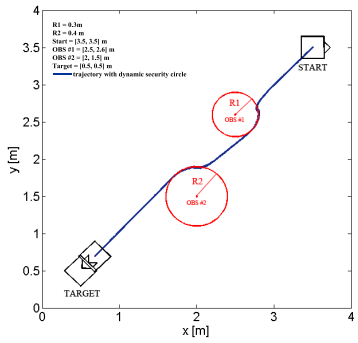

Fig. 7. Trajectory on x-y plane (case 2)

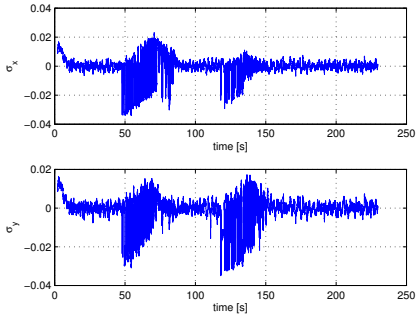

Fig. 8. Sliding surface for the position dynamics (case 2)

VII. Conclusions

In this paper a computational-efficient guidance algorithm based on the theory of artificial potential fields is proposed, combined with sliding mode techniques. A dynamic security radius of obstacle is proposed, to provide an algorithm that can be applied in real-time. Both a baseline scenario and multiple obstacles are analyzed. The experimental results in the base scenario with one obstacle prove the real-time feasibility of the proposed GC system. The efficiency of the algorithms, also in terms of the computational effort, is proven. Future works will be experimental results with a dynamic radius and with multiple obstacles.

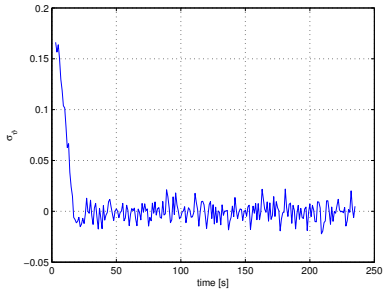

Fig. 9. Sliding surface for the attitude dynamics (case 2)

References

[1] Goodman, J. L., "History of space shuttle rendezvous and proximity operations," *Journal of Spacecraft and Rockets*, Vol. 43 (5), pp. 944-959, 2006.

[2] Emelyanov, S. V., *Variable structure control system (In Russian)*, Nauka, Moscow, 1967.

[3] Utkin, V. I., "Variable structure systems with sliding mode," *IEEE Trans Autom Control*, vol. 22 n. 2, pp. 212-222, 1977.

[4] Holguin, L., Prabhakaran Viswanathan, S., and Sanyal, A., "Guidance and Control for Spacecraft Autonomous Rendezvous and Proximity Maneuvers using a Geometric Mechanics Framework," *AIAA Guidance, Navigation, and Control Conference*, pp. 1-14, 2012.

[5] Sun, L. and Huo, W., "Robust Adaptive Control of Spacecraft Proximity Maneuvers under Dynamic Coupling and Uncertainty," *Advances in Space Research*, Vol. 56, pp. 2206-2217, 2015.

[6] McCamish, S.B., Romano, M., Nolet, S., Edwards, C.M., and Miller, D.W., "Flight Testing of Multiple Spacecraft Control on SPHERES During Close Proximity Operations," *AIAA Journal of Spacecraft and Rockets*, Vol. 46, No. 6, 2009.

[7] Lopez, I., and McInnes, C. R., "Autonomous Rendezvous using Artificial Potential Function Guidance," *Journal of Guidance, Control, and Dynamics*, Vol. 18(2), pp. 237-241, 1995.

[8] Zappulla II, R., Park, H., Virgili-Llop, J., and Romano, M., "Real-Time Autonomous Spacecraft Proximity Maneuvers and Docking Using an Adaptive Artificial Potential Field," *IEEE Transactions on Control Systems Technology*, accepted for Publication, to appear.

[9] Bloise, N., Capello, E., Dentis, M., and Punta, E, "Obstacle Avoidance with Potential Field Applied to a Rendezvous Maneuver," *Applied Sciences*, Vol. 7(10), pp. 1-16, 2017.

[10] Zappulla II, R., Virgili-Llop, J., Zagaris, C., Park, H., and Romano, M., "Dynamic Air-Bearing Hardware-in-the-Loop Testbed to Experimentally Evaluate Autonomous Spacecraft Proximity Maneuvers," *Journal of Spacecraft and Rockets*, Vol. 54 (4), pp. 825-839, 2017.

[11] Guldner, J. and Utkin, V. I., "Sliding Mode Control for Gradient tracking and Robot Navigation using Artificial Potential Fields," *IEEE Transactions on Robotics and Automation*, vol. 11, no. 2, pp. 247-254, 1995.

[12] Ge, S. S., and Cui, Y. J. , "New Potential Functions for Mobile Robot Path Planning," *IEEE Transactions on Robotics and Automation*," vol. 16 n. 5, pp. 615620, 2000.

[13] Utkin, V. I., *Sliding Modes in Optimization and Control Problems*, New York: Springer, 1992.

[14] Capello, E., Dabbene, F., Guglieri, G., Punta, E., and Tempo, R., "Sliding Mode Control Strategies for Rendezvous and Docking Maneuvers," *Journal of Guidance, Control and Dynamics*, vol. 40 n. 6, pp. 1481-1487, 2017.

[15] Bartolini, G., Ferrara, A. and Usai, E., "Chattering Avoidance by Second-order Sliding Mode Control," *IEEE Transactions on Automatic Control*, vol. 43(2), pp. 241-246, 1998.

[16] Levant, A., "Sliding Order and Sliding Accuracy in Sliding Mode Control," *International Journal of Control*, vol. 58(6), pp. 1247-1263, 1993.

[17] Sira-Ramrez, H., "Delta-Sigma Modulation". In: Sliding Mode Control. Control Engineering. Birkh auser, 2015.